WATER RESOURCES RESEARCH, VOL. 37, NO. 5, PAGES 1341–1350, MAY 2001

Testing a blowing snow model against distributed snow measurements at Upper Sheep Creek, Idaho, United States of America

Rajiv Prasad,[1,2] David G. Tarboton,[1] Glen E. Liston,[3] Charles H. Luce,[4] and Mark S. Seyfried[5]

Abstract. In this paper a physically based snow transport model (SnowTran-3D) was used to simulate snow drifting over a 30 m grid and was compared to detailed snow water equivalence (SWE) surveys on three dates within a small 0.25 km^2 subwatershed, Upper Sheep Creek. Two precipitation scenarios and two vegetation scenarios were used to carry out four snow transport model runs in order to (1) evaluate the blowing snow model, (2) evaluate the sensitivity of the snow transport model to precipitation and vegetation inputs, and (3) evaluate the linearity of snow accumulation patterns and the utility of the drift factor concept in distributed snow modeling. Spatial comparison methods consisted of (1) pointwise comparisons of measured and modeled SWE, (2) visual comparisons of the spatial maps, (3) comparisons of the basin-wide average SWE, (4) comparisons of zonal average SWE in accumulation and scour zones, and (5) comparisons of distribution functions. We found that the basin average modeled SWE was in reasonable agreement with observations and that visually the spatial pattern of snow accumulation was well represented except for a pattern shift. Pointwise comparisons between the modeled and observed SWE maps displayed significant errors. The distribution functions of SnowTran-3D-modeled drift factors from two precipitation scenarios on three dates were compared with the distribution function of observation-based drift factors obtained previously by calibration to evaluate the assumption of linearity. We found only a 14% reduction in explained variance in the distribution function of drift factors for a 69% increase in precipitation, suggesting that the simplification provided by the use of drift factor distributions will result in errors that are tolerable in many cases.

1. Introduction

The hydrologic response from northwestern U.S. rangelands is strongly influenced by snowmelt. The importance of snow drifting in the magnitude and timing of snowmelt water inputs during the hydrologic response has been well documented [*Cooley*, 1988; *Luce et al.*, 1997, 1998]. The spatial variability of surface water input from melting snowdrifts controls the magnitude and timing of runoff from these watersheds. One way of quantifying the spatial variability of snowpack is to conduct manual snow surveys throughout the winter. This is a costly endeavor and can only be used to sample small areas. Since measurements are impractical at larger scales, some form of modeling is needed. Apart from some specialized blowing-snow models [e.g., *Pomeroy and Gray*, 1995; *Liston and Sturm*, 1998] most physically based snow accumulation and melt models do not include a description of wind-driven drift; indeed, they are point models, and application of these models at the watershed scale needs to account for lateral snow exchanges. One way to accommodate wind-driven snow drift is to use manually measured snow water equivalence (SWE) surveys in association with a snow accumulation and melt model to derive drift factors [*Jackson*, 1994; *Tarboton et al.*, 1995; *Luce et al.*, 1998]. The drift factor at a point is a factor by which gage snowfall must be multiplied to equate measured and modeled SWE on the ground. It is used to describe the tendency of a location to accumulate extra snow through drifting (drift factor >1) or to lose snow due to scouring (drift factor <1). These drift factors vary spatially over the domain and are multiplied with observed snowfall to model snowfall redistribution by wind.

The purpose of this paper is to apply a blowing-snow model [*Liston and Sturm*, 1998], called SnowTran-3D, to portions of the Reynolds Creek Experimental Watershed (Figure 1) to estimate the spatial distribution of snowpack during the accumulation and drift period. This is a mass transport model which takes inputs of snowfall, air temperature, humidity, and wind speed and direction and models the effect of their interaction with topography and vegetation on the accumulation of wind-blown snow. This study addressed the following questions: (1) How well does SnowTran-3D simulate the spatial patterns of snow accumulation due to drifting? (2) How sensitive is the modeled pattern of snow accumulation to vegetation? (3) How sensitive are the model-derived drift factors to precipitation?

[1]Department of Civil and Environmental Engineering, Utah State University, Logan, Utah.
[2]Now at Pacific Northwest National Laboratory, Richland, Washington.
[3]Department of Atmospheric Science, Colorado State University, Fort Collins, Colorado.
[4]U.S. Forest Service, Department of Agriculture, Boise, Idaho.
[5]Northwest Watershed Research Center, Agricultural Research Service, U.S. Department of Agriculture, Boise, Idaho.

Copyright 2001 by the American Geophysical Union.

Paper number 2000WR900317.
0043-1397/01/2000WR900317$09.00

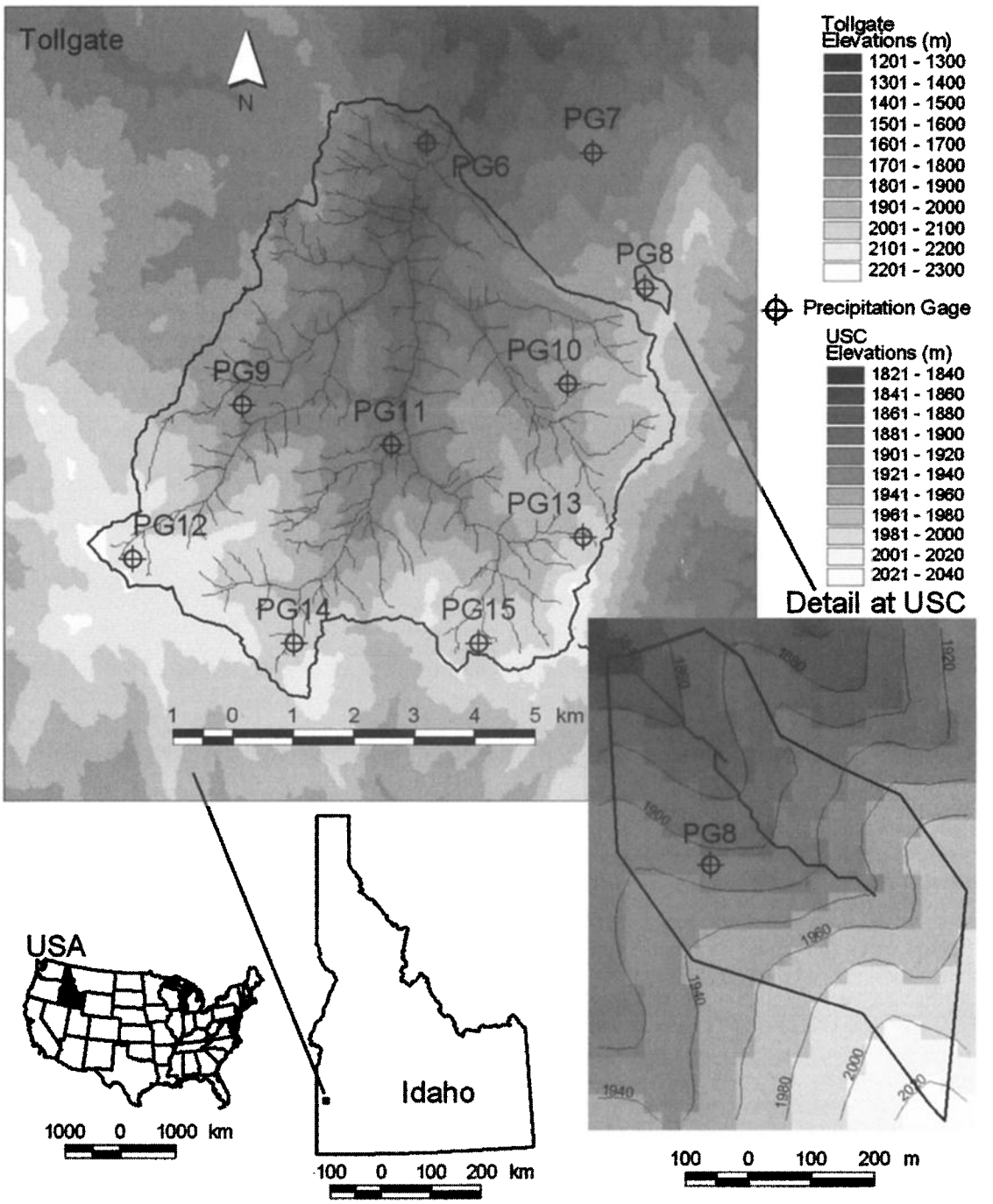

Figure 1. The study watersheds: Upper Sheep Creek (USC) is a 0.25 km^2 first-order subwatershed. Tollgate watershed is 54 km^2 in size. The underlying digital elevation model (DEM) is the 10 m resolution commercial DEM created from 1:24000 U.S. Geological Survey quad sheets.

The first question evaluates the performance of the blowing-snow model. The second question is of interest because although topography is now readily available in the form of digital elevation data, fine-scale vegetation maps are less commonly available. It is thus useful to know how important fine-scale vegetation information is in determining the spatial pattern of snow accumulation. The third question focuses on the validity and utility of the drift factor concept. The drift factor concept assumes linear scaling with amount of snowfall, so that with double the snowfall, accumulated snow amounts will be doubled while preserving the spatial pattern. We evaluate the validity of this assumption using SnowTran-3D model simulations.

2. Study Site and Available Data

Reynolds Creek Experimental Watershed (RCEW) is a semiarid mountainous watershed located in southwestern Idaho, United States of America, and has been the focus of intensive hydrologic instrumentation and investigation over

the last 3 decades [e.g., *Hamon*, 1973; *Stephenson and Freeze*, 1974; *Winkelmaier*, 1987; *Hanson*, 1989; *Duffy et al.*, 1991; *Stevens*, 1991; *Flerchinger et al.*, 1992]. The watershed is maintained by the Northwest Watershed Research Center (NWRC), Boise, Idaho, a part of the Agricultural Research Service, U.S. Department of Agriculture. This study focused on the 54 km^2 Tollgate and 0.25 km^2 Upper Sheep Creek (USC) watersheds (Figure 1) located within RCEW. Elevations in the Tollgate watershed range from 1403 to 2239 m. Mean annual precipitation varies with elevation and ranges from approximately 450 to over 1200 mm. Mean annual precipitation in USC is about 508 mm. The watershed is almost entirely sagebrush rangeland (87%) with some stands of Douglas fir, aspen, and alpine fir forest (13%). The hydrology of the watershed is mainly snowmelt driven. Channel flow is sustained by groundwater recharged by infiltration of snowmelt.

Upper Sheep Creek was the location of intensive study of the distribution of snow over the period 1982 to 1996. A 30 m grid over the watershed defines 255 locations where snowpack was measured at roughly 2 week intervals during the winter [*Cooley*, 1988]. In particular, nine snow surveys were conducted during water year 1992–1993, thereby establishing the spatio-temporal distribution of snow accumulation and melt at USC. Snow depth and SWE measurements were obtained using standard snow sampling techniques and the Rosen type snow sampler [*Jones*, 1983]. Each snow sample consisted of inserting the snow tube into the snowpack to the soil surface, recording the depth of the snowpack, removing the tube, and recording the SWE as the residual of the weight of the tube and snow sample minus the weight of the empty tube. Manpower limitations were such that it required two storm-free days to fully sample the complete 30 m grid. Maps of SWE measured by the first three of the snow surveys are shown in Figure 2.

Point data used in this study consisted of observed time series of precipitation, radiation, wind speed and direction, air temperature, and relative humidity. A commercial, high-resolution 10 m grid digital elevation model (DEM) was acquired from 1:24,000 U.S. Geological Survey quadrangle sheets for Reynolds Creek Experimental Watershed. In this study we used a 30 m DEM which was obtained by averaging the 10 m DEM to maintain consistency with the vegetation data which were available only at 30 m resolution. A Landsat 5 thematic mapper image acquired on August 1, 1993, was used to derive a plant community map using a maximum likelihood classification procedure. This vegetation map is shown in Figure 3. Hourly weather data including wind speed, global radiation, humidity and air temperature were measured at three stations in RCEW during 1992–1993. Wind direction, however, was available only at one station coinciding with PG7 (Figure 1). This study focused on the period October 1, 1992, to March 23, 1993, a single snow accumulation and drift season. Adjusted hourly precipitation data based on the dual-gage system described by *Hanson* [1989] for 15 gages in RCEW for 1992–1993 were provided by the NWRC. Measured precipitation can have significant uncertainty associated with it, especially in the context of estimation of spatial volume from a network of gages [see, e.g., *Hanson*, 1989; *Groisman and Legates*, 1994; *Morrissey et al.*, 1995; *McCollum and Krajewski*, 1998].

Eight of the precipitation gages were located inside Tollgate. The cumulative precipitation and cumulative snowfall amounts for this period for the eight gages located inside Tollgate, PG7 (outside Tollgate, located inside Lower Sheep Creek), and PG8 (outside Tollgate, located inside USC) are given in Table 1. All of these 10 gages are located inside the rectangular study area that includes Tollgate and USC watersheds (Figure 1). Snowfall was estimated based on air temperature using the relationship given by *U.S. Army Corps of Engineers* [1956]. There is an increasing trend in precipitation with elevation as well as a decreasing southwest-to-northeast trend. Among the gages in Table 1 the lowest precipitation during the study period occurred at PG7 (254.8 mm) and the highest occurred at PG12 (1067.3 mm). The amount of precipitation at USC (PG8), by comparison, was 555.8 mm during the same period. The simulation year 1992–1993 was above average in terms of precipitation (555.8 mm winter precipitation versus 508 mm of mean annual precipitation).

3. Snow Transport Model (SnowTran-3D)

A physically based snow transport model (SnowTran-3D) is described by *Liston and Sturm* [1998]. This is a three-dimensional mass-transport model, which includes processes related to snow captured by vegetation, topographic modification of wind speeds, snow cover shear strength, wind-induced surface shear stress, snow transport resulting from saltation and suspension, snow accumulation and erosion, and sublimation of blowing and drifting snow (Figure 4a). The model runs on a grid with variable vegetation cover and is driven by air temperature, humidity, wind speed and direction, and precipitation. The model outputs the time-evolving snow depth distribution over the simulation domain.

The fundamental equation in the snow transport model is the mass balance equation

$$\frac{d\zeta}{dt} = \frac{1}{\rho_s}\left[\rho_w P - \left(\frac{dQ_s}{dx} + \frac{dQ_t}{dx} + \frac{dQ_s}{dy} + \frac{dQ_t}{dy}\right) - Q_v\right], \quad (1)$$

where t is time (seconds), x (meters), and y (meters) refer to the horizontal spatial coordinates in west-east and north-south directions, respectively, ρ_s (kg m^{-3}) and ρ_w (kg m^{-3}) are densities of snow and water, respectively, Q_s (kg m^{-1} s^{-1}) and Q_t (kg m^{-1} s^{-1}) are the horizontal mass transport rates due to saltation and turbulent suspension, respectively, Q_v (kg m^{-1} s^{-1}) is the rate of sublimation of snow particles being transported, P (m s^{-1}) is precipitation in terms of water equivalence, and ζ (meters) is the snow depth. This neglects (or implicitly includes in ζ) the mass storage in suspended and saltating snow particles. The schematic of this mass balance accounting is shown in Figure 4b. Equation (1) is solved numerically over the simulation domain.

The shear stress that the wind exerts on the surface is used to parameterize snow transport by saltation and suspension. The shear stress is formulated in terms of the friction velocity u_* (m s^{-1}):

$$u_* = u_r \frac{\kappa}{\ln(z_r/z_0)}, \quad (2)$$

where u_r (m s^{-1}) is the wind speed at the reference height z_r (meters), z_0 (meters) is the surface roughness length (dependent on vegetation height and whether snow completely covers the vegetation), and κ is von Karman's constant.

The availability of snow for transport is determined by a snow-holding capacity parameter for each vegetation type. Only snow in excess of this capacity is available for wind transport.

The transport rate due to saltation is parameterized by

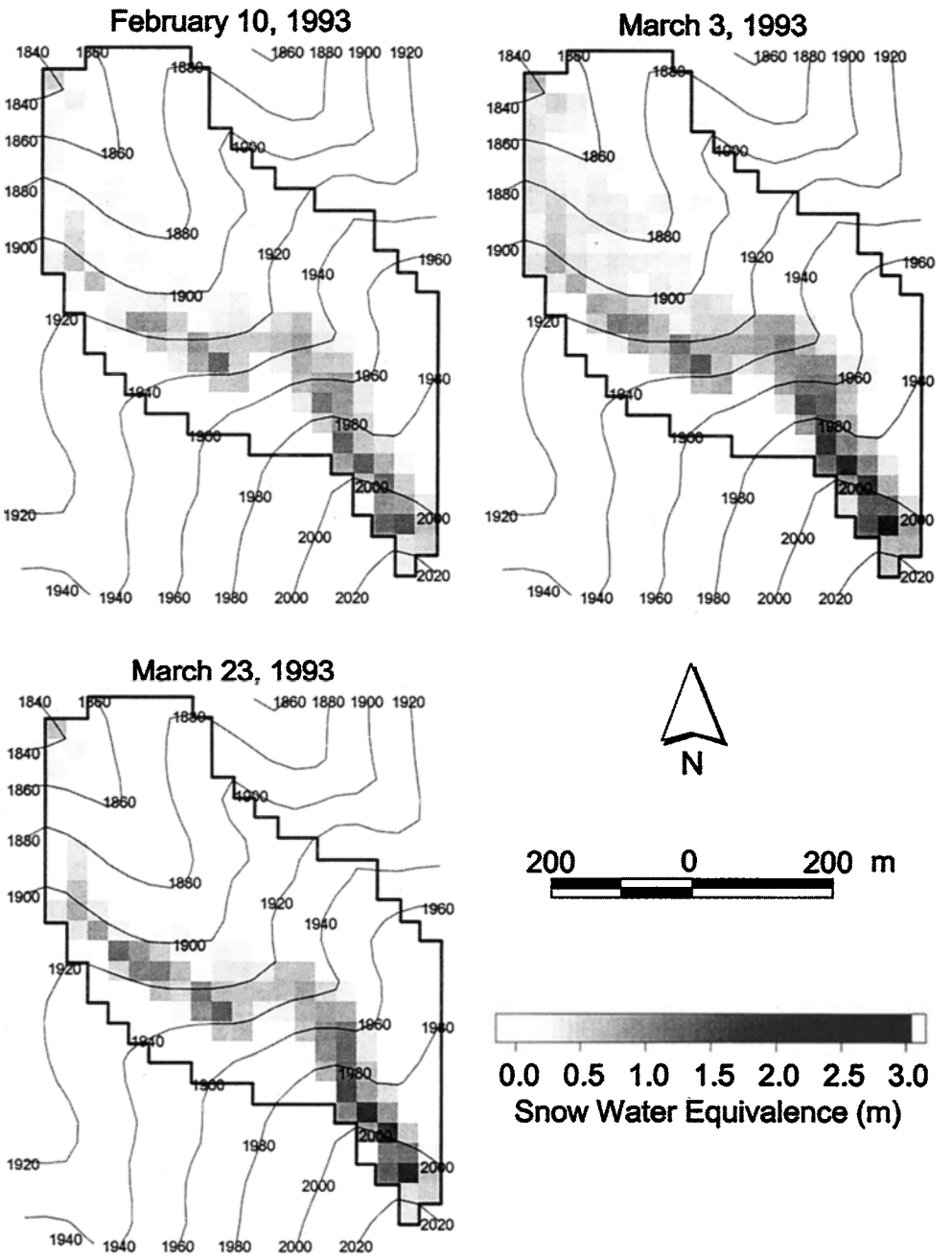

Figure 2. The snow water equivalence (SWE) measurements were carried out on a 30.48 m grid approximately aligned with the long axis of Upper Sheep Creek watershed. The maps were produced by interpolation of measured data on to the 30 m north aligned DEM grid. Contours give elevation in meters.

$$\frac{dQ_s(x^*)}{dx^*} = \frac{\mu}{f}(Q_{s_\max} - Q_s(x^*)) \qquad \frac{\partial u_*}{\partial x^*} \geq 0$$
$$Q_s(x^*) = \min\,[Q_s(x^* - \Delta x^*),\, Q_{s_\max}(x^*)] \qquad \frac{\partial u_*}{\partial x^*} < 0, \tag{3}$$

where x^* (meters) is the horizontal coordinate in a reference frame defined by the direction of wind flow (increasing downwind), Δx^* (meters) is the horizontal grid resolution, μ is a nondimensional scaling constant, f (meters) is the equilibrium fetch distance assumed to be somewhere between 300 m suggested by *Takeuchi* [1980] and 500 m adopted by *Pomeroy et al.* [1993], and $Q_{s_\max}$ (kg m^{-1} s^{-1}) is the saltation transport rate under equilibrium conditions [*Pomeroy and Gray*, 1990] given by

$$Q_{s_\max} = \frac{0.68}{u_*}(\rho_a/g)u_{*_t}(u_*^2 - u_{*_t}^2), \tag{4}$$

where u_{*_t} (m s^{-1}) is the threshold friction velocity, ρ_a (kg m^{-3}) is the density of air, and g (m s^{-2}) is the acceleration due to gravity.

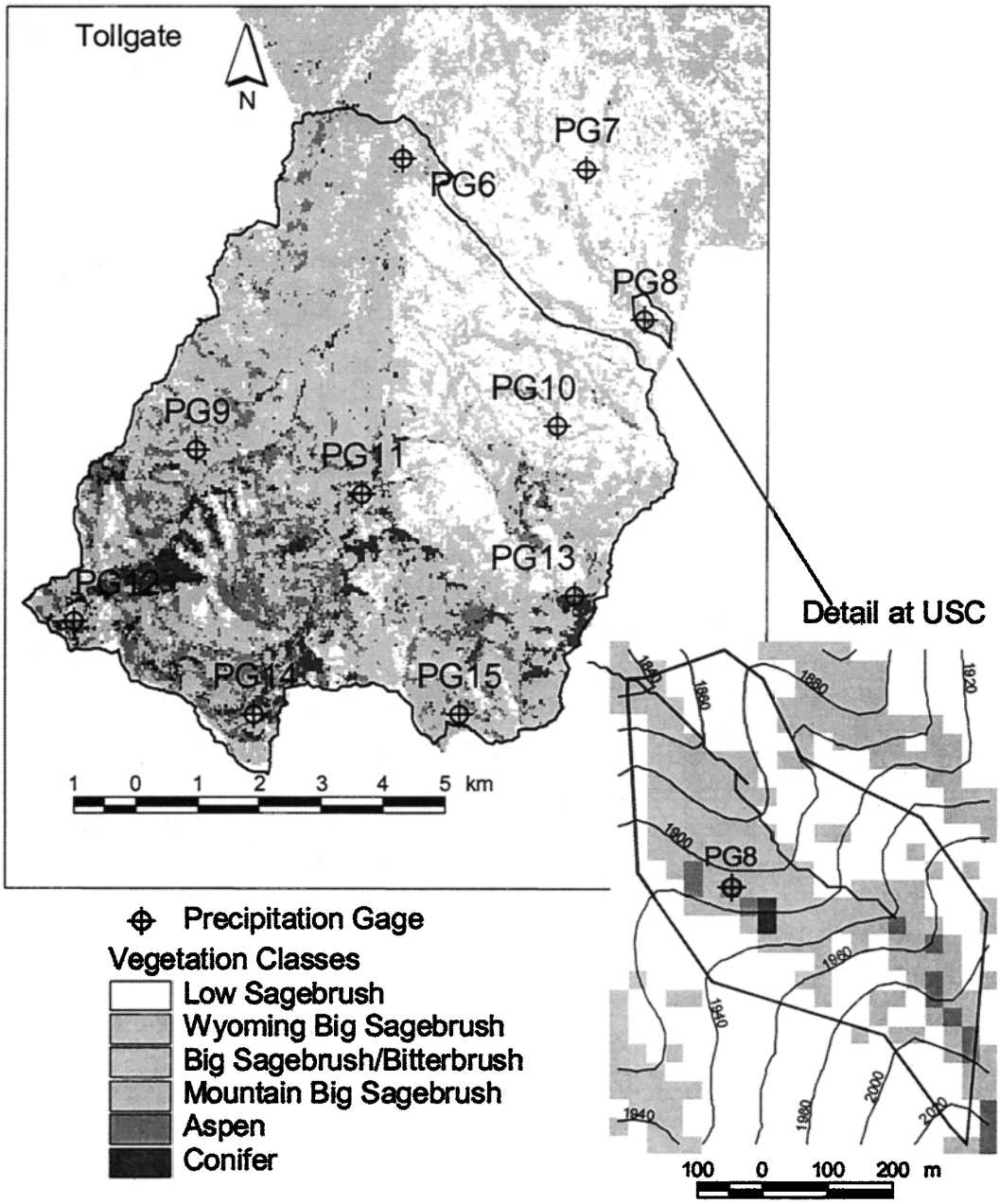

Figure 3. Vegetation map derived from Landsat 5 thematic mapper data for August 1, 1993, using a maximum likelihood classification. Note that the area outside the Reynolds Creek Experimental Watershed was masked out. For the model simulations we assumed that this outside area was covered by the most prevalent vegetation class, Mountain big sagebrush.

The transport rate due to turbulent suspension is given by

$$Q_t(x^*) = \int_{h*}^{z_t} \phi_t(x^*, z) u(x^*, z)\, dz, \tag{5}$$

where z (meters) is height above the snow surface, ϕ_t (kg m^{-3}) is the mass concentration of the particulate cloud, u (m s^{-1}) is the wind velocity, h_* (meters) is the height at the top of the saltation layer, and z_t (meters) is the height of the top of the turbulent-suspension layer, where the concentration is zero. The concentration of suspended snow ϕ_t is modeled using a particle settling velocity of 0.3 m s^{-1} [*Schmidt*, 1982] and the parameterization given by *Kind* [1992]. *Liston and Sturm* [1998] give full details.

During transport, snow particles are sublimated. The rate of sublimation during transport is much higher than that during nontransport conditions. The sublimation rate per unit area of snow cover is given by Q_v (kg m^{-2} s^{-1}):

$$Q_v(x^*) = \int_0^{z_t} \psi(x^*, z) \phi(x^*, z)\, dz, \tag{6}$$

where ψ (second^{-1}) is the sublimation loss rate coefficient and ϕ (kg m^{-3}) is the vertical mass concentration distribution. The

Table 1. Cumulative Precipitation in and Around Tollgate

Precipitation Station	Cumulative Precipitation October 1, 1992, to March 3, 1993, mm	Cumulative Snowfall October 1, 1992, to March 3, 1993, mm
PG6 (Tollgate)	258.8 (332.2)[a]	208.9 (237.9)
PG7 (Lower Sheep Creek)	206.2 (254.8)	163.1 (183.2)
PG8 (Upper Sheep Creek)	504.9 (555.8)	435.4 (450.3)
PG9 (Tollgate)	527.1 (693.4)	411.8 (459.9)
PG10 (Tollgate)	317.5 (387.6)	264.8 (289.6)
PG11 (Tollgate)	389.4 (522.0)	312.1 (353.7)
PG12 (Tollgate)	876.3 (1067.3)	735.8 (801.6)
PG13 (Tollgate)	598.4 (712.0)	510.2 (545.1)
PG14 (Tollgate)	649.7 (792.5)	545.5 (589.4)
PG15 (Tollgate)	744.5 (894.6)	634.3 (682.8)

[a]Numbers in parentheses are cumulative precipitation values for October 1, 1992, to March 23, 1993.

detailed formulation for sublimation loss rate coefficient ψ is given by *Liston and Sturm* [1998].

The wind field which drives the snow transport can be generated by several methods, which include (1) using a physically based, full atmospheric model (e.g., the Regional Atmospheric Modeling System [*Pielke et al.*, 1992; *Liston and Pielke*, 2000]) or a boundary layer circulation model [e.g., *Liston et al.*, 1993; *Liston*, 1995] which satisfy relevant momentum and continuity equations, (2) using an atmospheric model in which only mass continuity is satisfied [e.g., *Sherman*, 1978; *Ross et al.*, 1988], (3) interpolation using extensive (windward and leeward slope) wind speed and direction observations, and (4) interpolation using wind speed and direction observations in conjunction with empirical wind-topography relationships [e.g., *Ryan*, 1977]. Input wind speeds in the domain are interpolated to the modeling grid, and then the wind speed field u_r is modified to account for topographic variations by multiplying by an empirical weighting factor W, given by

$$W = 1.0 + \gamma_s\Omega_s + \gamma_c\Omega_c, \tag{7}$$

where Ω_s and Ω_c are topographic slope and curvature, respectively, in the direction of the wind and γ_s and γ_c are positive constants which weight the relative influence of the topographic slope and curvature, respectively, on modifying the wind speed. The slope and curvature are computed such that leeward and concave slopes produce Ω_s and Ω_c less than zero and windward and convex slopes produce Ω_s and Ω_c greater than zero. Values of γ_s (11) and γ_c (360) reported to be consistent with wind-microtopographic relationships [*Yoshino*, 1975] were used. In this study the last method was used because only a single wind speed and direction were available for input. This spatially uniform wind field was modified using (7) to estimate grid wind speeds.

4. SnowTran-3D Results

SnowTran-3D simulations were carried out over the 165 km^2 rectangular area surrounding and including the Tollgate and USC watersheds (see Figures 1 and 3). The buffer around the watershed accounts for snow sources and drift traps outside the watershed. This region was selected because our ultimate goal is to use the SnowTran-3D results to obtain drift factors for a hydrologic model over the Tollgate watershed. Detailed measurements are available only at Upper Sheep Creek, so the focus of this paper is on comparison with the detailed USC data.

The SnowTran-3D simulations included two vegetation scenarios, (1) vegetation derived from classification of the Landsat image and (2) uniform vegetation assuming the parameters of Mountain big sagebrush, the most common vegetation class, and two precipitation scenarios, (1) precipitation obtained

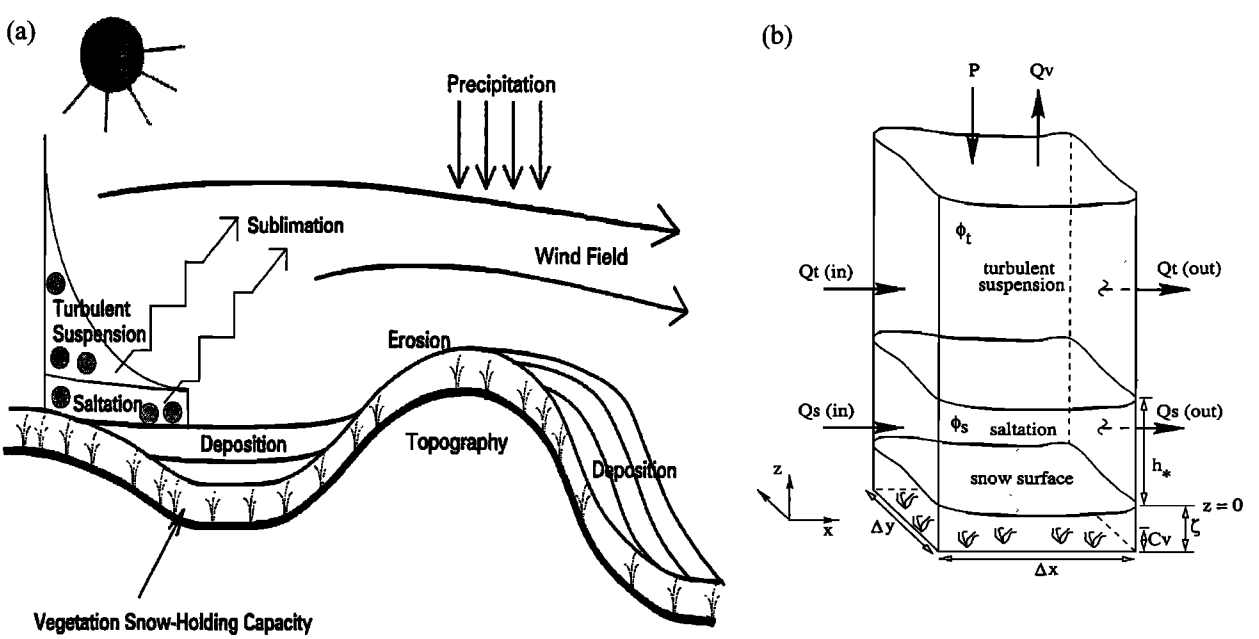

Figure 4. (a) Key features of the snow transport model (SnowTran-3D) [*Liston and Sturm*, 1998] as applied to topographically variable terrain. (b) Schematic of mass balance accounting in SnowTran-3D. Reprinted from the *Journal of Glaciology* with permission of the International Glaciological Society.

Table 2. Vegetation Properties for Tollgate Study Area Defined in Figure 1

Description	Height, m	Holding Capacity, m Depth	Holding Capacity, m SWE	Area Covered Within Tollgate Watershed, %
Low sagebrush	0.3	0.1	0.03	28.5
Wyoming big sagebrush	0.8	0.3	0.09	8.2
Big sagebrush/bitterbrush	0.8	0.3	0.09	13.9
Mountain big sagebrush	0.8	0.3	0.09	36.2
Aspen	4.0	1.0	0.3	7.3
Conifer	8.0	4.0	1.2	5.8

from the Upper Sheep Creek precipitation gage (PG8) which was near the lower end of the range of precipitation in Tollgate and (2) precipitation obtained from PG12 which had the highest mean annual precipitation and highest measured precipitation during the study period within Tollgate. The combination of these scenarios necessitated four SnowTran-3D model runs. The vegetation properties estimated for each vegetation class and used as input to SnowTran-3D are given in Table 2. Height for each vegetation community identified in Figure 3 was assigned an average based on field observation. Snow-holding capacity for each vegetation community was assigned based on subjective evaluation of properties of these communities with respect to blowing snow.

SnowTran-3D models snow depths with an assumed snow density, here taken as 300 kg m^{-3}. In the model, snow is available for transport only when the snow-holding capacity of vegetation has been exceeded. SnowTran-3D does not include parameterization of snow morphology processes such as densification. *Liston and Sturm* [1998] evaluated a simple densification parameterization within the model and did not find appreciable improvement in the accuracy of modeled snow cover, and the increase in model complexity was not justified.

SnowTran-3D was run at hourly time steps for the study duration using wind speeds measured at USC (PG8) and wind directions measured at PG7. PG7 was the only location where wind directions were measured, so these were used over the entire grid despite questions as to how representative they may be of the overall wind direction field.

Results from the four model input scenarios were analyzed for sensitivity of the snow transport model with respect to vegetation conditions and precipitation volume by comparison with the observations at USC. We compared measured and modeled SWE on the three survey dates of February 10, March 3, and March 23, 1993, prior to the onset of substantial snowmelt. The results were similar for all three dates, so, for brevity, only results from the date of peak accumulation (March 3,

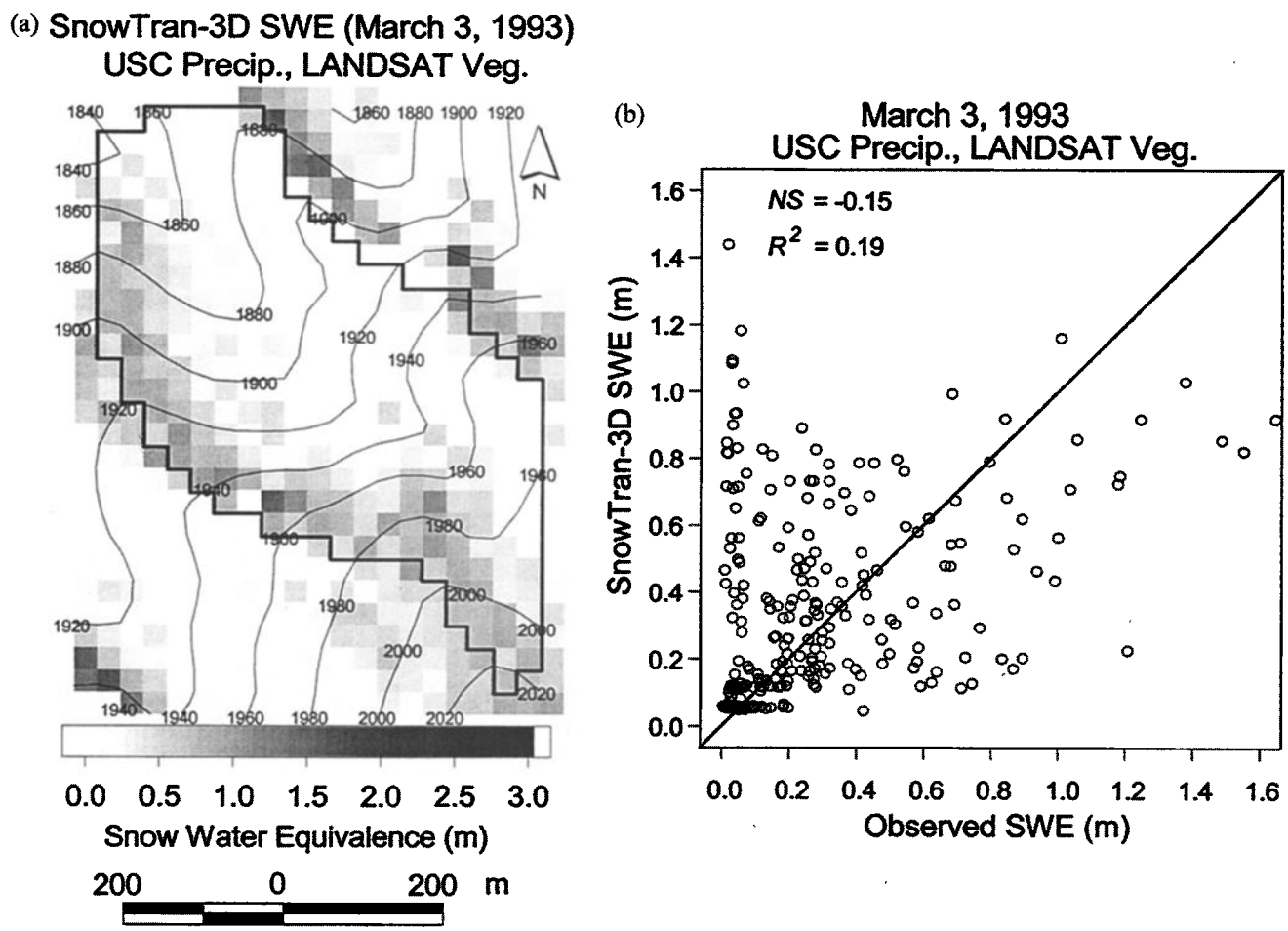

Figure 5. (a) SnowTran-3D-modeled snow water equivalence (SWE) map. Vegetation was obtained by classifying a Landsat image. (b) Pointwise comparison of modeled against observed SWE.

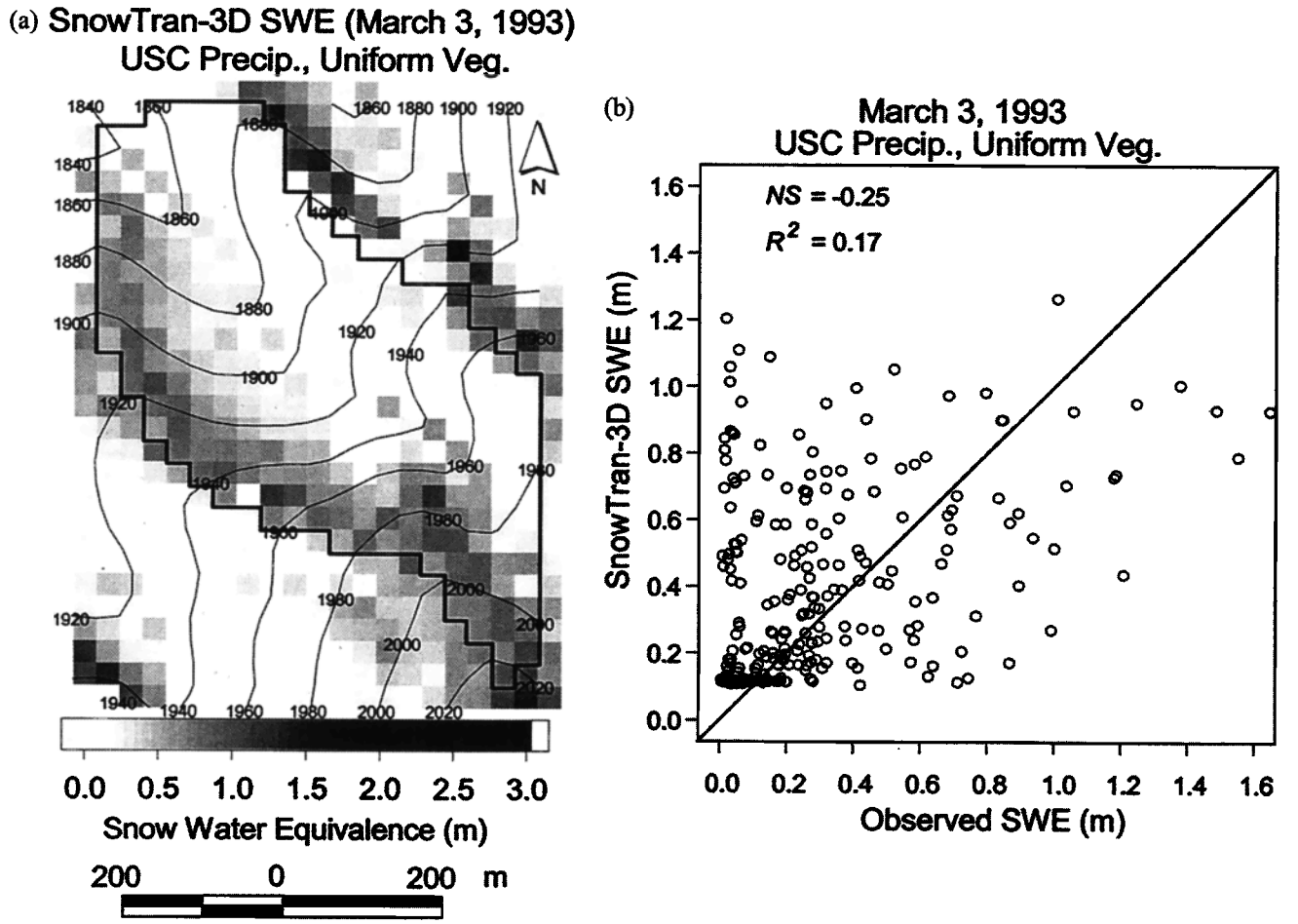

Figure 6. (a) SnowTran-3D-modeled SWE map. Mountain big sagebrush was used as uniform vegetation. (b) Pointwise comparison of modeled against observed SWE.

1993) are shown. Figure 5a shows the SWE map as modeled by SnowTran-3D using vegetation derived from the Landsat image in and around Upper Sheep Creek, and Figure 5b shows the scatterplot of modeled versus observed SWE at each grid cell in Upper Sheep Creek.

In modeled versus observed comparisons such as Figure 5b, the goodness of fit was quantified using the coefficient of determination R^2 from a linear regression of modeled versus observed SWE and the Nash-Sutcliffe measure [e.g., *Gupta et al.*, 1998]

$$\mathrm{NS} = 1 - \frac{\sum_{i=1}^{n} (\mathrm{SWE}^i_{\mathrm{obs}} - \mathrm{SWE}^i_{\mathrm{mod}})^2}{\sum_{i=1}^{n} (\mathrm{SWE}^i_{\mathrm{obs}} - \overline{\mathrm{SWE}}_{\mathrm{obs}})^2}, \qquad (8)$$

where $\mathrm{SWE}^i_{\mathrm{obs}}$ is the observed SWE at the ith location, $\mathrm{SWE}^i_{\mathrm{mod}}$ is the modeled SWE at corresponding location, $\overline{\mathrm{SWE}}_{\mathrm{obs}}$ is the mean observed SWE, and n is the number of grid cells comprising USC. This latter measure is preferable because it accounts for systematic as well as unsystematic differences between modeled and observed quantities. R^2 (from linear regression) quantifies only the error due to unsystematic differences. NS is scaled by the observed variance so it may be interpreted as representing the fraction of variance explained by the model (which may be negative for a poor model).

The NS measure for the comparison in Figure 5b was −0.15 (R^2 = 0.19). Figure 6 is similar to Figure 5, except that the vegetation used in this case consisted of spatially uniform Mountain big sagebrush, the most common vegetation class at Tollgate. The NS measure for the comparison in Figure 6b was −0.25 (R^2 = 0.17). Figure 7 shows the SWE maps modeled by SnowTran-3D runs using PG12 precipitation.

There is a discernible pattern mismatch between the observed and modeled SWE maps (see Figures 2, 5, 6 and 7), mainly responsible for the large scatter in the scatterplots in Figures 5b and 6b, and the correspondingly poor goodness of fit values. The observed drift on the leeward slope of Upper Sheep Creek forms approximately 30–60 m away from the watershed ridge (Figure 2). The modeled snow drift formed right up to the ridge of the watershed. These results indicate that in terms of pointwise comparisons the model performed poorly. We believe that the main reason for this discrepancy is that the model calculated wind speed based on a local estimate of terrain slope in the direction of the wind using the digital elevation data. This means that as soon as the computed slope is away from the wind (indicating a leeward slope), wind speed is reduced, leading to deposition of snow being carried by the wind. In reality, wind flowing over the terrain experiences flow separation, and deposition of snow occurs in the wake behind the ridges. A modeling approach that examines slope breaks rather than slope directly may be able to rectify some of these

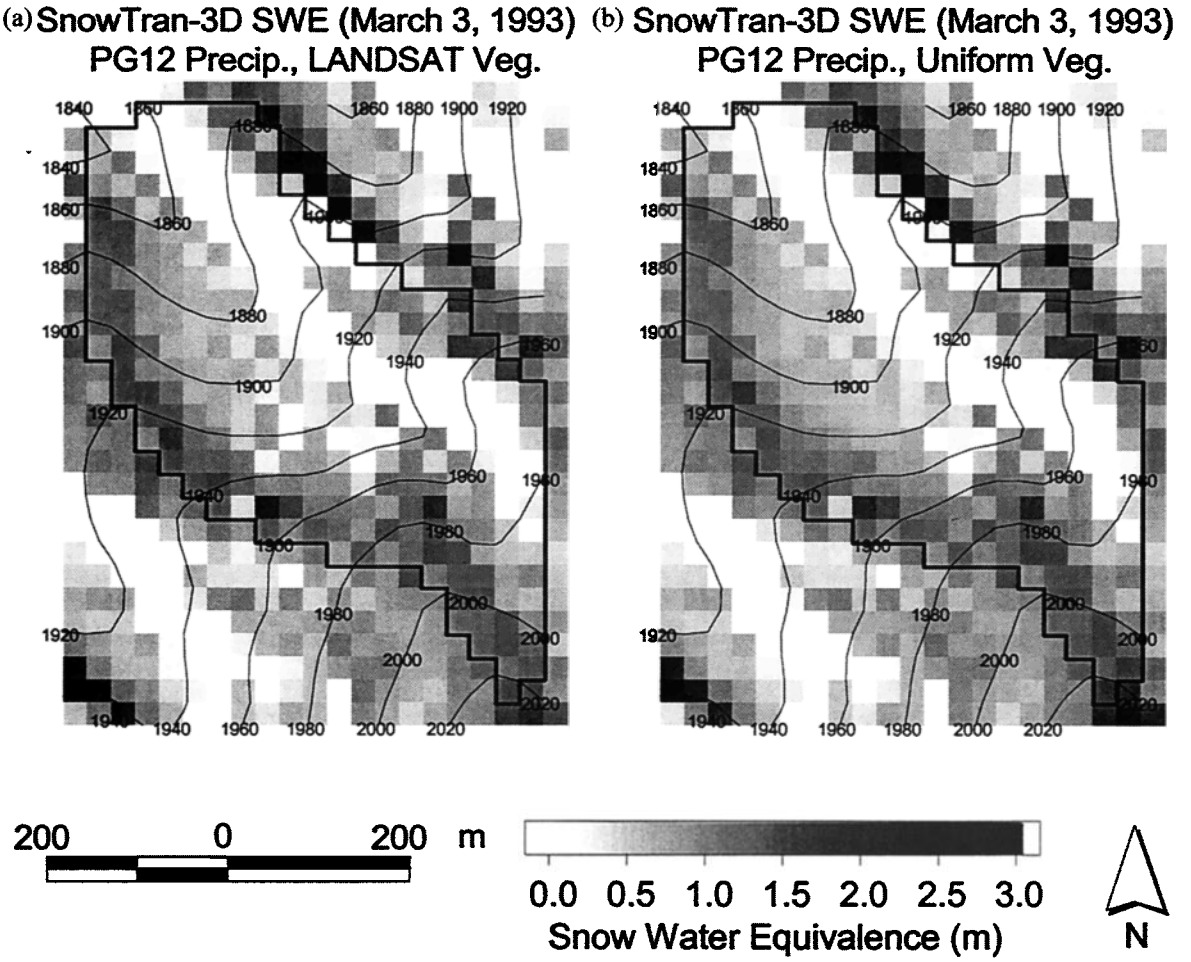

Figure 7. SnowTran-3D-modeled SWE maps at USC using PG12 precipitation. (a) Landsat vegetation scenario. (b) Uniform vegetation scenario.

problems. Currently, SnowTran-3D does not have this capability. The more advanced wind-modeling options within SnowTran-3D may also be better at representing flow separation but may also require more input data. Another reason for some of the discrepancy may be differences between wind direction as modeled (based on the measured wind direction at Lower Sheep Creek, PG7, Figures 1 and 3) and the true wind direction at Upper Sheep Creek.

Although the pointwise comparisons between measured and modeled accumulations (Figures 5b and 6b) show significant differences, the spatial pattern looks similar at a coarser scale. The patterns of accumulation with increased precipitation (Figure 7) also appear similar. In what follows, we test the performance of SnowTran-3D by comparisons of (1) the basin average SWE, (2) the scouring and accumulation on the erosion and deposition zones, respectively, in relation to snowfall amount, and (3) the distribution functions of SWE and drift factors, rather than individual points.

These tests are important because we intend to use the drift factors obtained by SnowTran-3D simulations to parameterize the distribution function of drift factors within watersheds for a watershed-scale hydrologic model. The distribution function of drift factors is used to partition the watershed into surface water input zones (R. Prasad et al., Understanding hydrologic behavior of a small semi-arid mountainous watershed, submitted to *Hydrological Processes*, 2000) (hereinafter referred to as Prasad et al., submitted manuscript, 2000), which is shown to be necessary in order to reproduce the timing of runoff from USC. In order for the drift factors obtained from SnowTran-3D to be effective in the above mentioned context, the distribution functions of the modeled and observation-based drift factors (described in section 4.1) must show reasonable agreement.

4.1. Drift Factors

Drift factors are intended to capture in a dimensionless way the propensity of a location to accumulate or lose snow by wind redistribution. Drift factors vary spatially over the domain but as applied practically are constant in time at each location. Drift factors are estimated by comparing either modeled or measured snow accumulation at each point to gage measured snowfall over the time period spanning snow accumulation.

When using measured snow accumulation, snowmelt during the accumulation and drift period, though relatively small, needed to be considered in the estimation of drift factors. Snowmelt was modeled at each grid cell using the Utah energy balance (UEB) snow accumulation and melt model, which is a physically based, energy balance model and operates on a one-layer snowpack at a point [*Tarboton et al.*, 1995; *Tarboton and Luce*, 1996] (Tarboton and Luce material available at

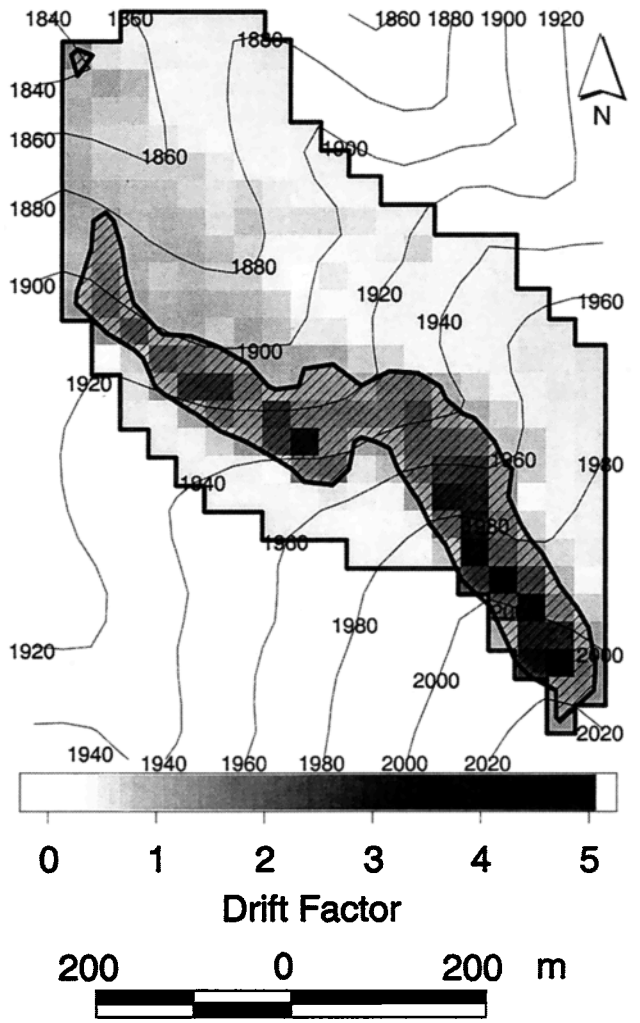

Figure 8. USC drift factors obtained by calibration. The hatched area is the observed deposition zone (drift factor ≥1), and the rest of the watershed is the erosion zone (drift factor <1).

http://www.engineering.usu.edu/dtarb/). Calibration of drift factors was carried out against observed SWE maps on the first three dates of SWE measurements (February 10, March 3, and March 23, 1993). The objective function used for each location during this calibration was the sum of signed differences between UEB-modeled and observed SWE on the three dates. With this objective function definition, negative and positive differences retain their sign so that when added they can cancel. The objective function can therefore be positive or negative and is optimum at zero when negative and positive differences exactly cancel. Because the drift factor only affects snowfall inputs, increases in drift factor must result in increases in modeled SWE. The objective function is therefore monotonic with respect to drift factor, and this fact was used to compute drift factor at each location as the value that made the objective function equal to zero. Other parameters of UEB were fixed at their recommended values [*Tarboton and Luce*, 1996]. The resulting drift factors (Figure 8) are henceforth referred to as observation-based drift factors.

Cumulative winter snowmelt until the date of peak accumulation as modeled by UEB was 0.039 m as compared to the cumulative snowfall of 0.435 m measured at USC. Because this snowmelt is small, any snowmelt model errors have a small effect on drift factor estimates. The UEB snowmelt model, drift factor concept, and snow distribution at USC have been the subject of several previous studies [*Jackson*, 1994; *Tarboton et al.*, 1995; *Luce et al.*, 1998, 1999; D. G. Tarboton et al., A grid-based distributed hydrologic model: Testing against data from Reynolds Creek Experimental Watershed preprint volume, American Meteorological Society Conference on Hydrology, Dallas, Texas, pp. 79–84, January 15–20, 1995]. The drift factors obtained from SnowTran-3D simulations are compared below with the observation-based drift factors.

Since SnowTran-3D does not model snowmelt, drift factors were obtained from the SnowTran-3D model simulations by normalizing modeled accumulated SWE for each grid cell in the computational domain by the amount of snowfall:

$$f_{\text{drift}}(\vec{x}) = \frac{\text{SWE}_{\text{mod}}(\vec{x})}{P_{\text{snow}}(\vec{x})}, \tag{9}$$

where $\text{SWE}_{\text{mod}}(\vec{x})$ is the modeled SWE and $P_{\text{snow}}(\vec{x})$ is the cumulative snowfall at location $\vec{x}$ over the simulation period.

4.2. Modeled Basin Average SWE

Figure 9 shows the basin average SWE from each SnowTran-3D simulation on the three dates (February 10, March 3, and March 23, 1993) and observed basin average SWE on these and following dates for USC. Figure 9 also shows the UEB-modeled basin average SWE computed using the observation-based drift factors. The SnowTran-3D simulations show more snow accumulation than observed (or modeled using UEB). This is because SnowTran-3D does not model snowmelt. To have comparable quantities, it is necessary to estimate this melt. The UEB-simulated cumulative melt was added to the observed SWE quantities (observed SWE Plus UEB melt) to have a quantity that is comparable to SnowTran-3D simulations.

On March 3 the peak measured basin average accumulation was 0.277 m and the modeled basin average SWE from SnowTran-3D with Landsat vegetation was 0.328 m, almost exactly equal to the observed SWE plus UEB melt of 0.329 m. (This exact coincidence is fortuitous because we have already seen poor pointwise comparisons.) On March 3 the modeled basin average SWE from SnowTran-3D with uniform vegetation was 0.362 m, about 10% more than the observed SWE plus UEB melt. The basin average SWE modeled by SnowTran-3D is greater for uniform vegetation as compared to the Landsat vegetation. This is due to the fact that the uniform vegetation used was Mountain big sagebrush, assigned a height of 0.8 m and a snow-holding capacity of 0.3 m snow depth (0.09 m SWE). At Upper Sheep Creek the dominant vegetation in the scour zones is low sagebrush, assigned a height of 0.3 m and a snow-holding capacity of 0.1 m snow depth (0.03 m SWE). The difference between the two runs thus was almost entirely due to the difference between the holding capacity of low sagebrush (Landsat vegetation scenario) and that of Mountain big sagebrush (uniform vegetation scenario). Mountain big sagebrush held more snow, thereby reducing scouring on the erosion zone compared to the Landsat vegetation scenario, resulting in greater basin average SWE. These differences are indicative of the sensitivity of the modeled basin-wide SWE to information on vegetation.

SnowTran-3D modeled a net loss of snow from USC for all scenarios. Total snowfall until the date of peak accumulation

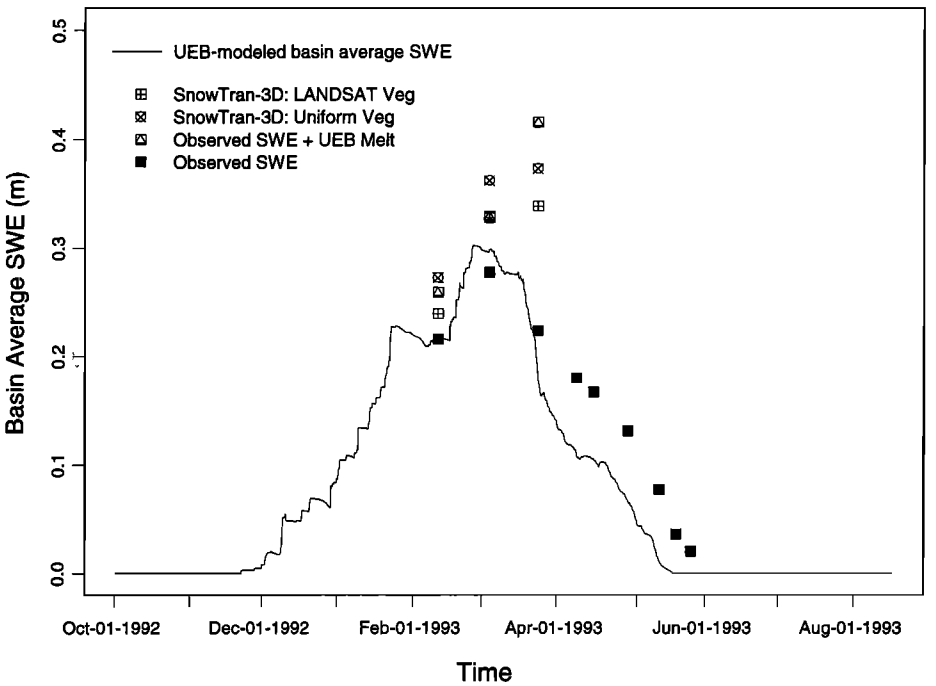

Figure 9. Comparison of SnowTran-3D predictions with observed SWE plus Utah Energy Balance (UEB) modeled melt at Upper Sheep Creek. SnowTran-3D used USC precipitation.

was 0.435 m for PG8 (USC) precipitation scenario. Of this amount, 0.333 m was the amount of modeled SWE in USC, and 0.05 m was modeled as lost because of sublimation for the Landsat vegetation scenario, resulting in a net transport of 0.052 m out of the watershed. The modeled basin average SWE on the date of peak accumulation for the uniform vegetation scenario was 0.367 m, and the modeled sublimation was 0.047 m, resulting in a net transport of 0.021 m out of the watershed. Since the vegetation holding capacity for uniform vegetation was greater than that for the Landsat vegetation scenario, it resulted in greater accumulation and less sublimation and less net transport loss. For the PG12 precipitation scenario the total amount of snowfall until the date of peak accumulation was 0.736 m. For the Landsat vegetation scenario, SnowTran-3D-modeled basin average SWE at USC was 0.618 m, and the modeled sublimation was 0.066 m, resulting in a net transport of 0.052 m out of the watershed. For the uniform vegetation scenario, basin average SWE was 0.638 m, and the modeled sublimation was 0.065 m, resulting in a net transport of 0.033 m out of the watershed.

The comparisons of measured versus modeled SWE presented here need to be viewed considering the uncertainty associated with precipitation inputs, which could be as large as the differences due to the vegetation scenarios compared. Although it is based on a comparison of only three dates, the general agreement of SnowTran-3D-modeled basin average SWE with the measured basin average SWE supports the adequacy of SnowTran-3D for modeling basin average SWE at USC.

4.3. Scouring and Accumulation Modeled by SnowTran-3D

In this section we examine the scouring on the erosion zone and the accumulation on the deposition zone of USC as observed and as modeled by SnowTran-3D. The erosion zone is defined as the set of grid cells where the drift factor (equation (9) and Figure 8) is less than 1. The deposition zone is defined as the set of grid cells where drift factor was greater than or equal to 1. The erosion and deposition zones observed and modeled for each scenario are slightly different because of the pointwise differences between observed and modeled accumulation patterns. Table 1 gives the cumulative precipitation and cumulative snowfall at USC during the drift and accumulation period for USC precipitation gage (PG8) and PG12 precipitation gage. Cumulative snowfall for the modeling period until peak accumulation (October 1, 1992, to March 3, 1993) at PG12 was 1.69 times that at PG8. Mean snow-holding capacities of vegetation on the observed erosion and deposition zones were 0.071 m and 0.093 m, respectively, with the Landsat vegetation. With uniform vegetation, mean snow-holding capacity was 0.09 m. The snow-holding capacities are expressed in terms of SWE. Snow is transported away from a location by SnowTran-3D only when accumulation exceeds the snow-holding capacity. Table 3 shows some statistics of the SWE on erosion and deposition zones at USC. Mean measured SWE on the erosion zone grew to its maximum of 0.129 m on the date of peak measured snow accumulation. Mean measured SWE on the deposition zone attained its maximum of 0.71 m on the day of peak measured accumulation.

The mean modeled SWE on the erosion zone for USC precipitation was greater (by about 23%) for the uniform vegetation compared to Landsat vegetation because of the greater snow-holding capacity of uniform vegetation. The corresponding increase in mean modeled SWE on the erosion zone for PG12 precipitation was about 5.5%. The mean modeled SWE on the deposition zone for USC precipitation was also greater (by about 3%) for the uniform vegetation compared to the Landsat vegetation. The corresponding increase in mean modeled SWE on the deposition zone for PG12 precipitation was about 1%.

Table 3. SWE on Erosion and Deposition Zones at Upper Sheep Creek[a]

	SWE on Erosion Zone on March 3, 1993	SWE on Deposition Zone on March 3, 1993
Observed		
Range, m	0.004–0.417	0.317–1.645
Mean, m	0.129	0.71
Standard Deviation, m	0.102	0.311
USC plus Landsat[b]		
Range, m	0.044–0.434	0.451–1.439
Mean, m	0.169	0.718
Standard Deviation, m	0.115	0.197
USC plus uniform[c]		
Range, m	0.104–0.666	0.458–1.265
Mean, m	0.208	0.740
Standard Deviation, m	0.124	0.191
PG12 plus Landsat[d]		
Range, m	0.060–1.498	0.681–1.765
Mean, m	0.421	1.083
Standard Deviation, m	0.305	0.216
PG12 plus uniform[e]		
Range, m	0.120–1.510	0.724–1.677
Mean, m	0.444	1.093
Standard Deviation, m	0.295	0.217

[a]The erosion zone is defined as the group of grid cells where the drift factor is less than 1, and the deposition zone is defined as the group of grid cells where the drift factor is greater than (or equal to) 1.
[b]Modeled with USC precipitation and Landsat vegetation.
[c]Modeled with USC precipitation and uniform vegetation.
[d]Modeled with PG12 precipitation and Landsat vegetation.
[e]Modeled with PG12 precipitation and uniform vegetation.

Table 4 shows the amount of snow scoured away from the erosion zone and the accumulation on the deposition zone. Amount of snow scoured away is computed by subtracting the SnowTran-3D-modeled mean SWE on the erosion zone from the cumulative snowfall. Amount of accumulation is computed by subtracting the cumulative snowfall from the SnowTran-3D-modeled average SWE on the deposition zone. The reduced scour for uniform vegetation on the erosion zone was due to the greater snow-holding capacity of the uniform vegetation as compared to that of Landsat vegetation. Note that when a larger quantity of precipitation was input, the modeled fraction that was scoured away reduced from around 60% to about 50%, while the modeled amount of scour in terms of SWE increased by about 25%. This analysis suggests that the quantity of snow redistributed is a function of both the available wind energy to transport snow (which was the same for both precipitation scenarios) and the amount of snow available to be transported. If available wind were the only limiting factor, we might have seen the same quantity of snow transported for both precipitation scenarios, and if available snow was the only limiting factor, we might have seen snow scoured down to the vegetation snow-holding capacity for both scenarios with correspondingly higher scour fraction for the higher-precipitation input scenario.

Table 4. Scouring and Accumulation on the Respective Zones at Upper Sheep Creek

	Amount of Snow Scoured or Accumulated Until March 3, 1993[a]
Observed	
Scour, m	0.307
Accumulation, m	0.267
USC plus Landsat[b]	
Scour, m	0.268 (62%)
Accumulation, m	0.277 (64%)
USC plus uniform[c]	
Scour, m	0.250 (58%)
Accumulation, m	0.273 (63%)
PG12 plus Landsat[d]	
Scour, m	0.395 (54%)
Accumulation, m	0.312 (42%)
PG12 plus uniform[e]	
Scour, m	0.379 (51%)
Accumulation, m	0.316 (43%)

[a]Scour is defined as (P_{snow} − mean SWE) on the erosion zone, and accumulation is defined as (mean SWE − P_{snow}) on the deposition zone. P_{snow} is cumulative snowfall. The values in parentheses indicate the percentage of cumulative snowfall scoured away from the erosion zone or the percentage of cumulative snowfall accumulated on the deposition zone.
[b]Modeled with USC precipitation and Landsat vegetation.
[c]Modeled with USC precipitation and uniform vegetation.
[d]Modeled with PG12 precipitation and Landsat vegetation.
[e]Modeled with PG12 precipitation and uniform vegetation.

In the deposition zone, although the modeled relative accumulation for Landsat vegetation scenario reduced from about 64% for USC precipitation to about 42% for PG12 precipitation, the modeled amount of snow accumulation in terms of SWE on the deposition zone increased by about 13%. This again suggests that the quantity of redistribution is a function of both available wind energy and available amount of snow. If wind were the only limiting factor, we would have seen the same amount of snow accumulation in terms of SWE for both precipitation scenarios.

4.4. Distribution Function Comparisons

In this section we evaluate the distribution functions of SWE and drift factors obtained from SnowTran-3D as compared to observations. Figures 5b and 6b gave pointwise comparisons, which were disappointing because of the spatial mismatch. Estimation of a large-scale surface water input (e.g., at the watershed scale) may not require precise pointwise agreement. Adequate results may be obtained if the distribution function of snow is well parameterized and used with the depletion curve concept as a subgrid parameterization [*Liston*, 1999; *Luce et al.*, 1999]. This section seeks to evaluate the extent to which the SnowTran-3D simulations are usable despite poor pointwise comparisons.

Figure 10 shows the cumulative distribution functions (CDF) of the observed and SnowTran-3D-modeled SWE for USC precipitation runs. The CDF from the Landsat vegetation scenario was closer to the observed than the CDF from the uniform vegetation scenario. The steps at the lower end of the CDF were due to the snow-holding capacities of low sagebrush (at 0.03 m) and taller sagebrush communities (0.09 m) on the windward slope. The CDF for uniform vegetation scenario showed only one step at around 0.09 m corresponding to the snow-holding capacity of uniform vegetation. Since SnowTran-3D does not model melt, the CDF for all scenarios started at values greater than 0. If snowmelt were modeled concurrently with snow transport, the CDF of modeled SWE would shift to the left, possibly resulting in better agreement with observed distribution function. Figure 11 shows the CDF of SWE modeled by SnowTran-3D at USC when precipitation from PG12 was used. Not surprisingly, the comparison with observed SWE distribution function was poor since the total

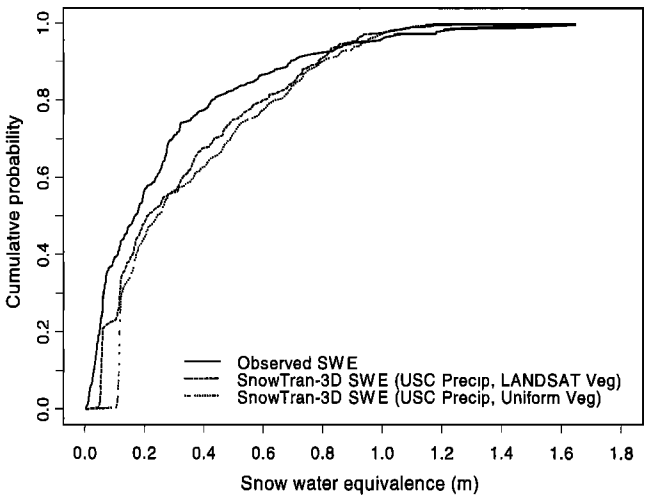

Figure 10. Comparison between cumulative distribution functions of observed and SnowTran-3D-modeled SWE at USC. SnowTran-3D used USC precipitation.

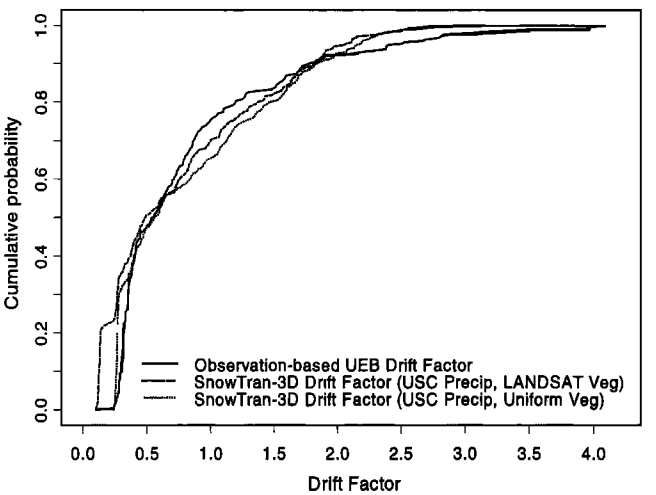

Figure 12. Comparison between cumulative distribution functions of observation-based and SnowTran-3D-modeled drift factors at USC. SnowTran-3D used USC precipitation.

amount of snowfall was different for the modeled distribution functions as compared to the observations.

To properly account for the spatially variable melting that occurred during the snow accumulation and drift period and to do this comparison in a dimensionless manner, we compared the distribution functions of observation-based drift factors and SnowTran-3D-modeled drift factors. The use of drift factors also allows us to estimate the sensitivity of SnowTran-3D distribution functions to precipitation inputs. The SnowTran-3D drift factors were computed for USC using (9) for all four scenarios. Figures 12 and 13 show the comparison between the CDF of drift factors at USC obtained from SnowTran-3D simulations with the CDF of observation-based drift factors. The agreement is generally quite good for both precipitation scenarios, indicating that the assumption of linearity as applied to the distribution function of drift factors with precipitation may not be bad. This observation was also suggested by *Liston* [1999]. Note however, that the distribution functions do degrade for PG12 precipitation, and a measure of the degradation is desirable.

In order to compare the distribution function of modeled and observed SWE, we plotted sorted modeled SWE against sorted observed SWE (Figure 14). A one-to-one line on these plots would indicate a perfect match between the distribution functions of modeled and observed SWE. For the data in Figure 14 we computed the NS goodness of fit measure (equation (8)). A value of 1 for NS would indicate a perfect match between the distribution functions of modeled and observed SWE. The distribution function of SWE obtained by the SnowTran-3D simulation which used USC precipitation and Landsat vegetation was quite good (NS = 0.90). The distribution function obtained from uniform vegetation scenario was slightly degraded but still quite good (NS = 0.83). Some of these differences may be due to uncertainty in precipitation inputs. Distribution functions of SWE obtained from PG12 precipitation runs had negative values for NS, which indicated that the sum of squares of errors was greater than the variance

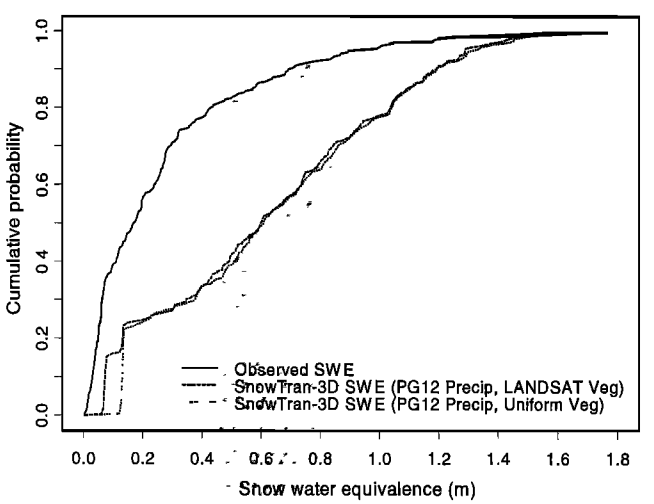

Figure 11. Comparison between cumulative distribution functions of observed and SnowTran-3D-modeled SWE at USC. SnowTran-3D used PG12 precipitation.

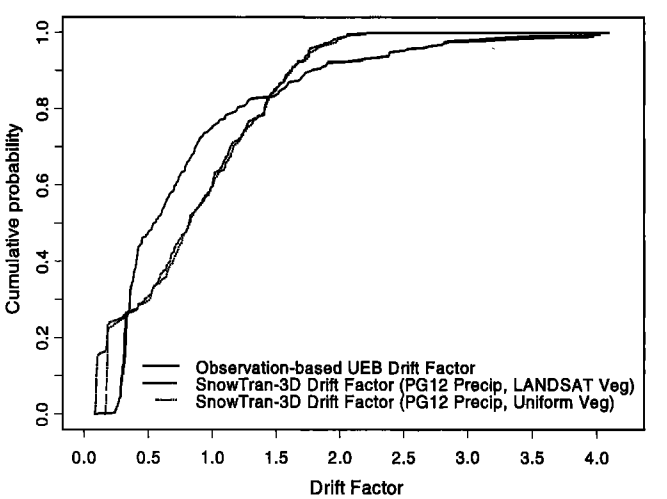

Figure 13. Comparison between cumulative distribution functions of observation-based and SnowTran-3D-modeled drift factors at USC. SnowTran-3D used PG12 precipitation.

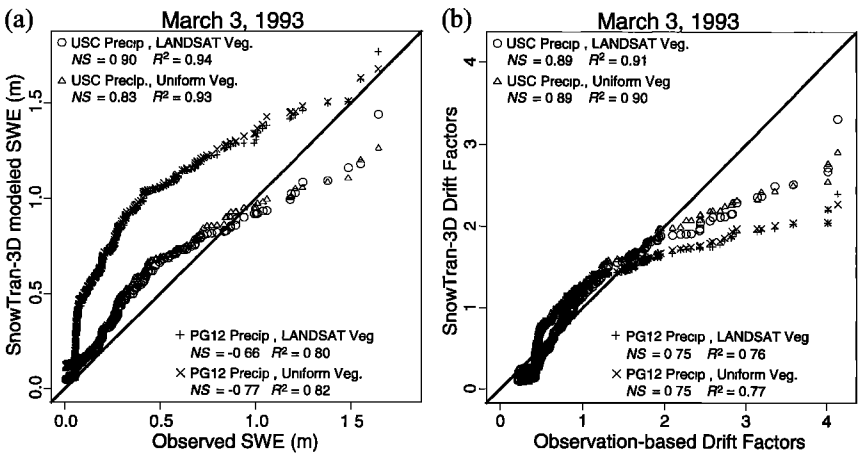

Figure 14. (a) Comparison between distribution functions of observed and SnowTran-3D-modeled SWE. Sorted modeled SWE is plotted against sorted observed SWE. The 1:1 line indicates perfect agreement between modeled and observed distribution functions of SWE. (b) Comparison between distribution functions of observation-based drift factors and SnowTran-3D-modeled drift factors. The plots are constructed in the same manner as in Figure 14a.

of observed SWE and that the modeled SWE was not comparable to observations, which is not surprising. The NS values were also computed for the drift factors by substituting observation-based UEB drift factors for observed SWE and SnowTran-3D modeled drift factors for modeled SWE in (8). The agreement between the distribution functions of SnowTran-3D modeled drift factors and observation-based drift factors was quite good when USC precipitation was used. The agreement worsend when precipitation from PG12 was used but not much (from about 0.89 for USC precipitation to about 0.75 for PG12 precipitation). This was also indicated by the closeness of the sorted drift factors plots in Figure 14b, where drift factors from all SnowTran-3D runs were close to each other.

Analysis of Figure 14 provides an answer to our third question, namely, how sensitive the drift factors were to the amount of precipitation in the context of the distribution function of drift factors. Our test of the drift factor concept used the precipitation from USC (PG8) and PG12 to compare the distribution functions of modeled drift factors for each of these cases to the distribution function of observation-based drift factors. The precipitation at PG12 was 69% more than that at USC (PG8). The significance of using PG12 as input was as a convenient and representative increased precipitation input (lacking a year of data at USC with significantly increased precipitation to simulate) rather than its geographic distance. There was also the question of the need for spatial precipitation interpolation, and by using the maximum (most different) value as a uniform input, we could evaluate the possible error due to inaccuracy in precipitation input due to interpolation and other errors and uncertainties.

The distribution functions of drift factors obtained from the SnowTran-3D simulations using USC precipitation were in good agreement with the observation-based drift factors for both vegetation scenarios. With the observed precipitation, SnowTran-3D-modeled drift factors explain 89% of the variance in the distribution function of observation-based drift factors. The fraction of explained variance reduced to 75% when precipitation from PG12 was used, resulting in a 14% reduction in explained variance of the distribution function of drift factors obtained from SnowTran-3D simulations for a precipitation increase of 69%. With the original (USC/PG8) precipitation, there was 11% error (unexplained variance), so the error (unexplained variance) is only increased to 25% with the additional 69% precipitation.

Though the agreement with the distribution function of observation-based UEB drift factors is not perfect (indicated by the nonlinearity of the sorted drift factors plots on Figure 14), it is deemed reasonably good. Some of the discrepancies may be due to factors discussed earlier in this section, notably the pattern mismatch, wind flow separation problems, and the lack of melt estimation as part of the snow transport modeling.

5. Conclusions

The first question addressed in this study asked how well the spatial patterns of snow accumulation due to drifting was represented by the blowing snow model. Basin average SWE was in reasonably good agreement with observed SWE plus estimated melt (see Figure 9). The pattern of SWE modeled by the snow transport model was similar to measured SWE maps (see Figures 2, 5a, 6a and 7), but pointwise comparisons showed significant errors (see Figures 5b and 6b), which could be attributed to the spatial mismatch and limitations of wind flow separation modeling. The analysis of scouring and accumulation on the scouring and deposition zones (Tables 3 and 4) showed that available wind as well as available snow played a role in limiting the amount of redistribution of snow.

The second question addressed by this study asked how sensitive the modeled pattern of snow accumulation was to vegetation. The snow held on the erosion zone was more sensitive to vegetation snow-holding capacity than that held on the deposition zone. As the amount of precipitation increased, this effect became relatively smaller. However, overall, in terms of drift factor distributions the differences between Landsat and uniform vegetation scenarios were insignificant. This suggests that, in this watershed at least, topography plays a more dominant role than vegetation in the determination of drift distributions and that efforts to map vegetation for the purposes of quantifying snow drift distributions are not critical. In other regions of the world (or in other landscapes), vegetation dis-

tributions can play a stronger role than topography in defining snow drift distributions [*Hiemstra*, 1999; *Liston et al.*, 2001; *Sturm et al.*, 2001].

The third question asked how sensitive the drift factors were to the amount of precipitation. The drift factor concept is analogous to an assumption of linearity. It assumes that if snowfall is increased, the amount of accumulated SWE will be increased while the spatial pattern due to drifting will be the same. If this approximation were reasonable, it would allow a separation between the modeling of snow drifting and that of snowmelt and surface water input. This is a significant simplification in model structure, especially when large watersheds must be modeled. Our test of this concept used the precipitation from USC (PG8) and PG12 to compare the distribution functions of modeled drift factors for each of these cases to the distribution function of observation-based drift factors. There was only a 14% reduction in the amount of explained variance for a 69% increase in precipitation. This error is small and in our opinion probably comparable to or less than many of the other errors, such as uncertainty in precipitation, that hydrologic modelers need to deal with. Thus the simplifications provided by the use of distribution functions of drift factors will be appropriate in many cases. These results have significant implications for hydrologic models that operate at the watershed scale and do not need precise pointwise agreement for parameterization of wind-induced drift (e.g., see Prasad et al., submitted manuscript, 2000).

In the context of upscaling of hydrologic models we need to upscale the description of snow accumulation and melt processes. There are practical difficulties associated with running point snowmelt models at the grid scale, even if we can adequately approximate the wind redistribution of snow using the drift factors concept. Recent attempts to describe the process of snow accumulation and melt using a depletion curve concept is a promising approach [*Liston*, 1999; *Luce et al.*, 1999]. Future work will involve modeling of hydrology at Tollgate using surface water input derived from (1) the UEB run at the grid scale with SnowTran-3D drift factors and (2) depletion curve method applied to first-order subwatersheds of Tollgate. This surface water input will be used to drive a three-zone hydrologic model (Prasad et al., submitted manuscript, 2000) to simulate annual water balance at Tollgate.

Acknowledgments. We appreciate the thoughtful reviews and suggestions of Günter Blöschl, Kelly Elder, and two anonymous WRR reviewers. This work was supported by the Environmental Protection Agency (agreement R824784) under the National Science Foundation/ Environmental Protection Agency Water and Watersheds program. The views and conclusions expressed are those of the authors and should not be interpreted as necessarily representing the official policies, either expressed or implied, of the U.S. government.

References

Cooley, K. R., Snowpack variability on western rangelands, paper presented at Western Snow Conference, Kalispell, Mont., April 18–20, 1988.

Duffy, C. J., K. R. Cooley, N. Mock, and D. Lee, Self-affine scaling and subsurface response to snowmelt in steep terrain, *J. Hydrol.*, *123*, 395–414, 1991.

Flerchinger, G. N., K. R. Cooley, and D. R. Ralston, Groundwater response to snowmelt in a mountainous watershed, *J. Hydrol.*, *133*, 293–311, 1992.

Groisman, P. Y., and D. R. Legates, The accuracy of United States precipitation data, *Bull. Am. Meteorol. Soc.*, *75*, 215–227, 1994.

Gupta, H. V., S. Sorooshian, and P. O. Yapo, Toward improved calibration of hydrologic models: Multiple and noncommensurable measures of information, *Water Resour. Res.*, *34*(4), 751–763, 1998.

Hamon, W. R., Computing actual precipitation, in *Proceedings of WMO-IDHS Symposium, Distribution of Precipitation in Mountainous Areas, Geilo, Norway, Rep. 326*, pp. 159–174, World Meteorol. Organ., Geneva, 1973.

Hanson, C. L., Precipitation catch measured by the Wyoming shield and the dual-gage system, *Water Resour. Bull.*, *25*, 159–164, 1989.

Hiemstra, C. A., Wind redistribution of snow at treeline, Medicine Bow Mountains, Wyoming, M.S. thesis, 163 pp., Univ. of Wyo., Laramie, 1999.

Jackson, T. H. R., A spatially distributed snowmelt-driven hydrological model applied to the Upper Sheep Creek Watershed, Ph.D. dissertation, 323 pp., Utah State Univ., Logan, 1994.

Jones, E. B., Snowpack ground-truth manual, *Rep. CR 170584*, NASA Goddard Space Flight Cent., Greenbelt, Md., 1983.

Kind, R. J., One-dimensional aeolian suspension above beds of loose particles—A new concentration-profile equation, *Atmos. Environ.*, *26A*(5), 927–931, 1992.

Liston, G. E., Local advection of momentum, heat, and moisture during the melt of patchy snow covers, *J. Appl. Meteorol.*, *34*, 1705–1715, 1995.

Liston, G. E., Interrelationships among snow distribution, snowmelt, and snow cover depletion: Implications for atmospheric, hydrologic, and ecologic modeling, *J. Appl. Meteorol.*, *38*, 1474–1487, 1999.

Liston, G. E., and R. A. Pielke Sr., A climate version of the regional atmospheric modeling system, *Theor. Appl. Climatol.*, *66*, 29–47, 2000.

Liston, G. E., and M. Sturm, A snow-transport model for complex terrain, *J. Glaciol.*, *44*(148), 498–516, 1998.

Liston, G. E., R. L. Brown, and J. Dent, Application of the $E - \varepsilon$ turbulence closure model to separated atmospheric surface layer flows, *Boundary Layer Meteorol.*, *66*, 281–301, 1993.

Liston, G. E., J. P. McFadden, R. A. Pielke Sr., and M. Sturm, Sensitivity of snowcover, energy, and moisture interactions to increased Arctic shrubs, *Global Change Biol.*, in press, 2001.

Luce, C. H., D. G. Tarboton, and K. R. Cooley, Spatially integrated snowmelt modeling of a semi-arid mountain watershed (abstract), *Eos Trans. AGU*, Fall Meet. Suppl., *78*(46), F205, 1997.

Luce, C. H., D. G. Tarboton, and K. R. Cooley, The influence of the spatial distribution of snow on basin-averaged snowmelt, *Hydrol. Processes*, *12*(10–11), 1671–1683, 1998.

Luce, C. H., D. G. Tarboton, and K. R. Cooley, Subgrid parameterization of snow distribution for an energy and mass balance snow cover model, *Hydrol. Processes*, *12*(10–11), 1671–1683, 1999.

McCollum, J. R., and W. F. Krajewski, Uncertainty of monthly rainfall estimates from rain gauges in the Global Precipitation Climatology Project, *Water Resour. Res.*, *34*(10), 2647–2654, 1998.

Morrissey, M. L., J. A. Maliekal, J. S. Greene, and J. Wang, The uncertainty in simple spatial averages using rain gauge networks, *Water Resour. Res.*, *31*(8), 2011–2017, 1995.

Pielke, R. A., et al., A comprehensive meteorological modeling system—RAMS, *Meteorol. Atmos. Phys.*, *49*, 69–91, 1992.

Pomeroy, J. W., and D. M. Gray, Saltation of snow, *Water Resour. Res.*, *26*(7), 1583–1594, 1990.

Pomeroy, J. W., and D. M. Gray, Snowcover: Accumulation, relocation and management, *Sci. Rep. 7*, Natl. Hydrol. Res. Inst., 144 pp., Saskatoon, Sask., Canada, 1995.

Pomeroy, J. W., D. M. Gray, and P. G. Landine, The prairie blowing snow model: Characteristics, validation, operation, *J. Hydrol.*, *144*, 165–192, 1993.

Ross, D. G., I. N. Smith, P. C. Manins, and D. G. Fox, Diagnostic wind field modeling for complex terrain: Model development and testing, *J. Appl. Meteorol.*, *27*, 785–796, 1988.

Ryan, B. C., A mathematical model for diagnosis and prediction of surface winds in mountainous terrain, *J. Appl. Meteorol.*, *16*, 571–584, 1977.

Schmidt, R. A., Vertical profiles of wind speed, snow concentration, and humidity in blowing snow, *Boundary Layer Meteorol.*, *34*, 213–241, 1982.

Sherman, C. A., A mass-consistent model for wind fields over complex terrain, *J. Appl. Meteorol.*, *17*, 312–319, 1978.

Stephenson, G. R., and R. A. Freeze, Mathematical simulation of subsurface flow contributions to snowmelt runoff, Reynolds Creek Watershed, Idaho, *Water Resour. Res.*, *10*(2), 284–294, 1974.

Stevens, G. R., A geophysical investigation of the Upper Sheep drain-

age, Reynolds Creek Experimental Watershed, Owyhee County, Idaho, Master's thesis, 119 pp., Geophys. Program, Univ. of Idaho, Moscow, 1991.

Sturm, M., J. P. McFadden, G. E. Liston, F. S. Chapin III, C. H. Racine, and J. Holmgren, Snow-shrub interactions in Arctic tundra: A hypothesis with climatic implications, *J. Clim.*, *14*(3), 336–344, 2001.

Takouchi, M., Vertical profiles and horizontal increases of drift snow transport, *J. Glaciol.*, *26*(94), 481–492, 1980.

Tarboton, D. G., and C. H. Luce, Utah energy balance snow accumulation and melt model (UEB), computer model technical description and users guide, Utah Water Res. Lab., Logan, 1996.

Tarboton, D. G., T. G. Chowdhury, and T. H. Jackson, A spatially distributed energy balance snowmelt model, in Biogeochemistry of Seasonally Snow-Covered Catchments, edited by K. A. Tonnessen et al., *IAHS Publ.*, *228*, 141–155, 1995.

U.S. Army Corps of Engineers, Snow hydrology, summary report of the snow investigations, N. Pac. Div., Portland, Oreg., 1956.

Winkelmaier, J. R., Ground-water flow characteristics in fractured basalt in a zero-order basin, master's thesis, 128 pp., Hydrol. Dep., Univ. of Idaho, Moscow, 1987.

Yoshino, M. M., *Climate in a Small Area*, 549 pp., Univ. of Tokyo Press, Tokyo, 1975.

G. E. Liston, Department of Atmospheric Science, Colorado State University, Fort Collins, CO 80523. (liston@atmos.colostate.edu)

C. H. Luce, Forest Service, U.S. Department of Agriculture, Boise, ID 83702. (cluce@fs.fed.us)

R. Prasad, Pacific Northwest National Laboratory, P.O. Box 999, MSIN K9-33, Richland WA 99352. (rajv.prasad@gte.net)

D. G. Tarboton, Department of Civil and Environmental Engineering, Utah State University, Logan, UT 84322. (rpras@cc.usu.edu; dtarb@cc.usu.edu)

M. S. Seyfried, Northwest Watershed Research Center, Agricultural Research Service, U.S. Department of Agriculture, Boise, ID 83712. (mseyfrie@nwrc.ars.pn.usbr.gov)

(Received February 22, 2000; revised September 13, 2000; accepted October 6, 2000.)